Digestive and Liver Disease 51 (2019) 1446–1455

Contents lists available at ScienceDirect

Digestive and Liver Disease

journal homepage: www.elsevier.com/locate/dld

Liver, Pancreas and Biliary Tract

circZFR promotes cell proliferation and migration by regulating miR-511/AKT1 axis in hepatocellular carcinoma

Xin Yang[a,*,1], Ling Liu[b,1], Heng Zou[a], Yan-Wen Zheng[a], Kun- Peng Wang[a]

[a] Department of General Surgery, The Second Xiangya Hospital, Central South University, Changsha, PR China
[b] Department of Hepatobiliary and Pancreatic Surgery, Xiangya Hospital, Central South University, Changsha, PR China

ARTICLE INFO

Article history:
Received 5 December 2018
Accepted 15 April 2019
Available online 28 May 2019

Keywords:
AKT1
circZFR
Hepatocellular carcinoma
Migration
miR-511
Proliferation

ABSTRACT

Background: Emerging data suggest the crucial regulatory roles of circular RNAs (circRNAs) in hepatocellular carcinoma (HCC). However, the pathophysiology role of circZFR in HCC remains largely unknown.
Aims: This study aims to disclose the functions of circZFR in HCC progression and its potential molecular mechanism.
Methods: circZFR and miR-511 were identified by qRT-PCR. Colony formation assay, wound-healing assay, transwell assay, and flow cytometry assay were performed to determine the cell proliferation, migration, invasion and apoptosis. Western blotting and immunohistochemistry (IHC) were utilized to evaluate the expression level of AKT1, GSK3β, β-catenin and cascades of proliferation-related proteins both *in vitro* and *in vivo*. Dual luciferase reporter assay was conducted to evaluate the interactions among circZFR, miR-511 and AKT1.
Results: The expression of circZFR was enhanced and the expression of miR-511 was down-regulated in HCC tissues and cells. Functionally, circZFR silencing or miR-511 overexpression suppressed cell proliferation, migration and invasion, and induced apoptosis of HCC cells. Mechanistically, circZFR acted as a miR-511 sponge to up-regulate its target gene AKT1, which activated cascades of proliferation-related proteins (c-Myc, cyclin D1, Survivin and Bcl-2). Furthermore, depletion of circZFR inhibited tumorigenesis and decreased the expression level of AKT1 in xenograft models.
Conclusion: circZFR promotes HCC progression by directly down-regulating miR-511 to activate AKT1 signaling, suggesting that circZFR is a potential target in HCC treatment. Targeting circZFR may provide therapeutic benefits for HCC.

1. Introduction

Hepatocellular carcinoma (HCC) is the fifth most common cancer with the second leading cause of cancer-related mortality worldwide [1]. Approximately 250,000 people die from HCC each year, with China accounting for about 45% [2]. The 5-year survival rate for patients with advanced HCC is only about 10% [3], which is largely attributed to the lack of reliable tools for early diagnosis [4]. Thus, it is a key prerequisite to identify reliable disease biomarkers to improve future treatment options.

As a novel class of non-coding RNAs, circular RNAs (circRNAs) that form circular structures through the joining of 3' and 5' terminals [5] have attracted great interest because of their potential therapeutic and diagnostic value in cancer [6]. Increasing evidence demonstrates that the aberrant expression of circRNAs may function as a key modulator of the tumor initiation and progression through targeting key genes [7]. In the context of HCC, several individual circRNA have been identified. For instance, a noteworthy down-regulation of circMTO1, cSMARCA5 and circZKSCAN1 were closely associated with suppression of cell proliferation and invasion [8–10]. On the other hand, enhanced expression of circHIPK3, has_circ_0016788, and circRNA100338 exerted tumor-promoting effects [11–14]. While increased expression of circZFR (hsa_circ_0072088) has been implicated in HCC progression [15], the exact function and molecular mechanisms remain largely unknown.

Micro RNAs (miRNAs) are a family of small non-coding RNAs that is known to play important regulatory roles in tumorigenesis [16]. Furthermore, a variety of studies have shown that miRNAs are important regulators of HCC development and progression [17–19].

* Corresponding author at: Department of General Surgery, The Second Xiangya Hospital, Central South University, No.139, Middle Renmin Road, Changsha 410011, Hunan Province, PR China.
E-mail address: yangxin6358@163.com (X. Yang).
[1] These are co-first authors.

https://doi.org/10.1016/j.dld.2019.04.012
1590-8658/

miR-511, an intronic miRNA encoded by both mouse and human *MRC1* genes [20], was aberrantly expressed in several human cancers, including HCC [21–25]. Depending on the cellular context, miR-511 can function either as an oncogene or as a tumor suppressor. In the context of HCC, majority studies suggested that miR-511 was frequently down-regulated and functions as a tumor inhibitor [23–25]. While accumulative evidence demonstrated that circZFRs could serve as sponges for miRNAs and thus regulate the function of miRNAs in HCC tumorigenesis [26], little is known about the circZFR-mirR-511 interaction in HCC.

miRNAs control multiple biological processes by blocking translation or by inducing the degradation of the target mRNAs. The serine-threonine protein kinase AKT1 is known to be hyperactivated in the majority of human cancers and contributes to tumorigenesis [27]. Furthermore, AKT1 was identified as unfavorable prognostic factors for HCC patients [28], and its hyperactivation was implicated in HCC initiation and progression [29,30]. The functional interaction between miRNA and AKT1 has been increasingly recognized. For example, miR-149 and miR-105 have been reported to serve as tumor suppressors by regulating the AKT1-mTOR or PI3K/AKT1 signaling pathway in HCC [29,30]. miR-511 expression has been found to correlate with AKT/mTOR signaling in HCC cell lines [24]. However, the underlying molecular mechanism, with special regard to the involvement of circRNA, remains to be determined.

In the current study, we identified that circZFR was significantly up-regulated in HCC tissues and cell lines and negatively correlated with miR-511 expression. In addition, circZFR promoted cell proliferation, migration and invasion of HCC cells and altered the expression of cascades of proliferation-related factors through targeting miR-511 and up-regulating its target gene AKT1. This is the first study to provide evidence of a functional interplay among circZFR, miR-511 and AKT1 in HCC tumorigenesis, thereby demonstrating the therapeutic potential of circZFR/miR-511/AKT1 axis for HCC.

2. Materials and methods

2.1. Clinical tissue samples

Thirty patients pathologically diagnosed as hepatocellular carcinoma (HCC) without receiving chemotherapy or radiotherapy before surgery were enrolled in this study. HCC tissue samples and adjacent non-tumor tissue samples were collected and immediately frozen in liquid nitrogen or at −80 °C. The study protocol was approved by the Ethics Committee of Xiangya Hospital of Central South University, with informed consent obtained from all patients.

2.2. Cell culture

HCC cell lines HepG2, Bel-7402, SMMC-7721, and Huh-7 and the human normal hepatic cell (WRL-68) were purchased from American Type Culture Collection (Manassas, VA, USA). HepG2 and WRL-68 cells were cultured in Dulbecco's modified Eagle medium (DMEM) while Bel-7402, SMMC-7721 and Huh-7 cells were cultured in RPMI-1640 (Thermo Fisher Scientific, USA). The medium was supplemented with 10% fetal bovine serum (FBS; Gibco, Grand Island, USA) and 1% penicillin–streptomycin (Invitrogen, CA, USA), and maintained at 37 °C in a humidified atmosphere containing 5% CO_2.

2.3. Cell transfection

Small hairpin RNAs (shRNAs) targeting circZFR (sh-circZFR) and miR-511 mimics and inhibitor were designed and synthesized by GenePharma (Shanghai, China). HCC cells were transfected with sh-NC, sh-circZFR, miR-511 mimics, mimics NC, miR-511 inhibitor, and inhibitor NC using Lipofectamine 3000 (Invitrogen, Eugene, OR, USA) according to the manufacturer's protocol. After 48 h of transfection, cells were harvested for the following experiments.

2.4. Wound-healing assay

The transfected HepG2 and Huh-7 cells were seeded into six-well plates and cultured overnight. Wounds were created in the center of each cell using a sterile 200 μL plastic pipette tips. Cells were then washed with culture medium and incubated for 24 h in serum-free medium. The wound was imaged at 0 and 24 h. Images were obtained under a microscopy (Olympus, Tokyo, Japan) at 40× magnification.

2.5. Transwell migration and invasion assay

Cells in serum-free medium were placed into the upper chamber of the 24-well transwell chambers, and medium containing 10% FBS was added into the lower chamber as chemoattractant. After incubation for 24 h at 37 °C, cells remaining on the upper chamber were removed with cotton wool, whereas cells adhering to the lower chamber were fixed in 1% paraformaldehyde, stained in a day solution with 0.5% crystal violet and counted. For the invasion assay, the upper chamber was coated with extracellular matrix (BD Biosciences, USA), a soluble basement membrane matrix. The rest of the assay was performed as the migration assay. The HCC cells of migration and invasion were counted and photographed in at least five random fields under a light microscopy (Olympus Corporation, Tokyo, Japan).

2.6. Colony formation assay

HCC cells were plated in 6-well plates. After incubation for 2 weeks in culture medium with 10% FBS, the medium was removed and the cells were stained with crystal violet for 30 min. Visible colonies were counted under a light microscopy. All assays were repeated three times.

2.7. Annexin V and PI staining for apoptosis

HCC cells were incubated with trypsin and washed with PBS twice. Upon resuspended in a solution containing 5 μL of Annexin V-FITC and 5 μL of PI (Dead Cell Apoptosis Kit, Thermo Fisher Scientific) and harvested in the dark for 15 min at 37 °C, the cells were analyzed on FACSCalibur machine (BD Biosciences, CA, USA) for the percentage of Annexin V^+PI^+ apoptotic cells.

2.8. RNA extraction and quantitative real time-polymerase chain reaction (qRT-PCR)

Total RNA was isolated from cells and tissues with TRIzol reagent (Invitrogen, Carlsbad, CA, USA). To determine the miRNA expression levels, complementary DNA was synthesized with random primers using the qScript microRNA cDNA Synthesis Kit (Quantabio, Beverly, MA). Quantitative real-time PCR (qRT-PCR) analysis was carried out using Bulge-Loop miRNA qRT-PCR Starter Kit (RiboBio), with U6 serving as an internal control gene. To quantify the expression levels of circZFR and mRNAs, 1 μg RNA was reverse transcribed into complementary DNA using Prime Script RT reagent Kit (Takara Bio, Shiga, Japan). Reactions were incubated in a 96-well optical plate at 95 °C for 5 min, followed by 40 cycles at 95 °C for 15 s and 60 °C for 1 min. All reactions were run in triplicate with 7500 real-time PCR System (Applied Biosystems, Foster City, CA, USA) using SYBR Premix Ex Taq II (TaKaRa). The following primer sequences were used: circZFR forward 5'-TGCCACCATTTATCCAACTG-3' and reverse 5'-CCACTCGCAAAACTCCTTTC-3'; miR-511 forward 5'-GCCCGTGTCT-

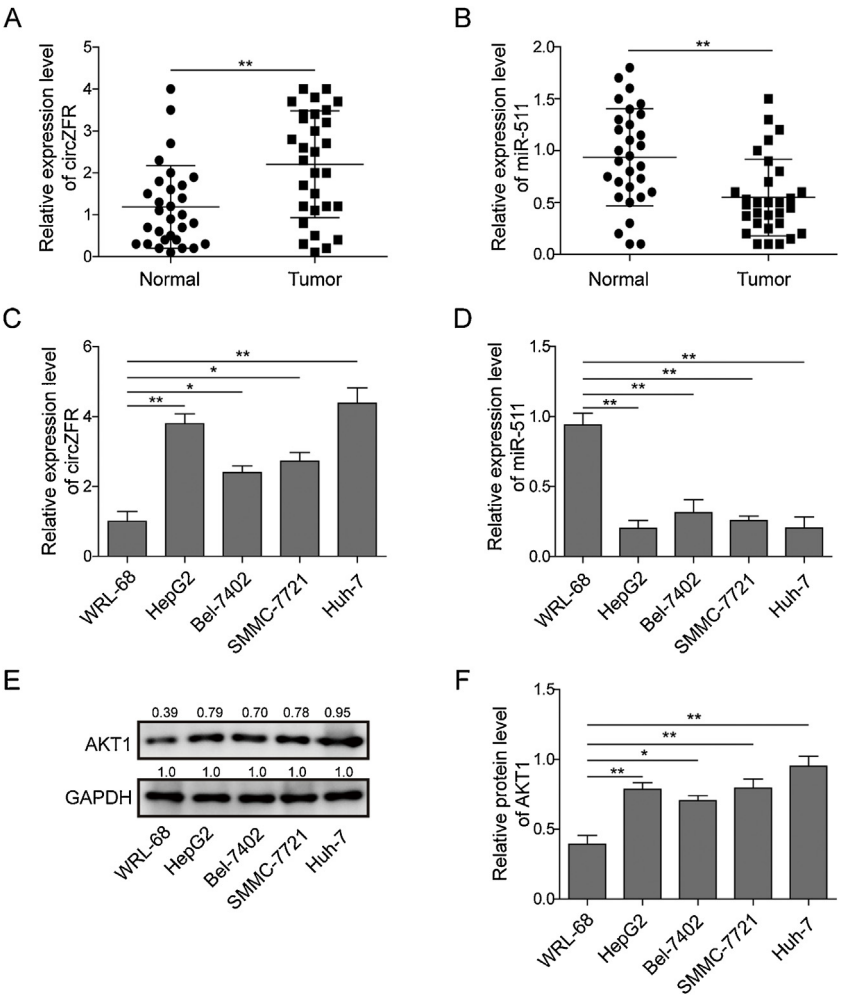

Fig. 1. Expression pattern of circZFR, miR-511, and AKT1 in HCC tissues and cells. The expression level of circZFR (A) and miR-511 (B) was detected by qRT-PCR in HCC tissues and adjacent normal tissues. The expression level of circZFR (C) and miR-511 (D) was detected by qRT-PCR in diverse HCC cell lines including HepG2, Bel-7402, SMMC-7721, and Huh-7, as compared with normal human hepatic cell line WRL-68. (E) Protein level of AKT1 was detected by western blotting in HCC cell lines and WRL-68 cells. (F) The quantification of relative protein level as a ratio to that of GAPDH (internal control). The results from cell experiments were shown as mean ± SD (n = 3), which were three separate experiments performed in triplicate. * = $p < 0.05$ and ** = $p < 0.01$.

TTTGCTCTG-3', and reverse 5'-GTCGTATCCAGTGCAGGGTCCGAG-GTATTCGCACTGGATACGACTGACTG-3'; AKT1 forward 5'-GCACCT-TCCATGTGGAGACT-3', and reverse 5'-GGGACACCTCCATCTCTTCA-3'; U6 (internal control for miRNAs) forward 5'-CTCGCTTCGG-CAGCACA-3', and reverse 5'-AACGCTTCACGAATTTGCGT-3' and GAPDH (internal control for mRNAs) forward, 5'-CCAGGTGGTCTCC-TCTGA-3' and reverse 5'- GCTGTAGCCAAATCGTTGT-3'. The $2^{-\Delta\Delta Ct}$ method was used to calculate the relative expression of targets.

2.9. Western blot analysis

Cultured cells were harvested and lysed in ice-cold radio immunoprecipitation assay buffer (RIPA, Beyotime, Beijing, China) supplied with 0.001% protease inhibitor cocktail (Roche, Pleasanton, CA, USA) and incubated on ice for 30 min. BCA Protein assay kit (Beyotime, Bejing, China) was then used to detect the concentrations of protein samples. Equal amounts of protein extracts were run on a 10% SDS-PAGE gels and transferred to polyvinylidene fluoride membranes (Milipore, Shanghai, China). The membranes were blocked with 5% nonfat milk, followed by incubation with primary antibodies at 4 °C overnight. Primary antibodies used were: rabbit anti-AKT1 antibody (1:500 dilution; #ab179463, Abcam), rabbit anti-GSK-3β antibody (1:5000 dilution; #ab32391), rabbit anti-p-GSK-3β antibody (1:1000 dilution; #9336, Cell Signaling, MA, USA), rabbit anti-β-catenin antibody (1:5000 dilution; #ab32572), rabbit anti-p-β-catenin antibody (1:1000 dilution; #a4176, Cell Signaling), rabbit-anti-Cyclin D1 antibody (1:10,000 dilution; #ab134175), rabbit anti-c-Myc antibody (1:1000 dilution; #ab32072), rabbit anti-Survivin antibody (1:5000 dilution; #ab76424), rabbit anti-Bcl-2 antibody (1:1000 dilution; #ab32124), and rabbit anti-GAPDH antibody (1:500 dilution; #ab9485). After being washed with PBS, the membrane was probed with corresponding goat anti-rabbit IgG H&L secondary antibodies (1:2000 dilution; #ab6721) at room temperature for 1 h. Finally, the protein signals were visualized by densitometry using an enhanced chemiluminescence detection kit (ECL, Thermo Scientific, Shanghai, China).

2.10. Immunohistochemistry (IHC)

The tissues were routinely fixed in 4% formalin and embedded in paraffin, and were sectioned at 4 μm thick. After being baked at 60 °C for 2 h, the tissues were incubated with xylene for deparaffinization and decreasing concentrations of ethanol for rehydration. Antigen retrieval was subsequently performed, and 3% hydrogen peroxide was applied to block endogenous peroxidase activity for 20 min. The sections were treated with normal goat serum to avoid nonspecific staining and incubated with the following primary anti-

bodies overnight at 4 °C: AKT1 (1:100 dilution; #ab179463, Abcam) antibody. The complex was visualized with DAB complex, and the nuclei were counterstained with haematoxylin. Positive immunostaining was assessed by proportion of positive cells.

2.11. Dual luciferase reporter assay

For luciferase reporter assay, the circZFR or AKT1 3'-UTR was amplified by PCR and inserted into the pGL3 luciferase promoter plasmid (Promega Corporation, Madison, WI, USA). Point mutations of the miR-511 targeting sites in the circZFR or AKT1 3'-UTR were generated using the QuickChange Multiple Site-directed Mutagenesis Kit (Stratagene, La Jolla, CA). HepG2 and Huh-7 cells were seeded in 12-well plates and each cell was subsequently co-transfected with miR-511 mimics, mimic NC, miR-511 inhibitor, inhibitor NC and luciferase plasmids using the Lipofectamine 2000 method (Invitrogen, Carlsbad, CA, USA). After 48 h of transfection, cell lysates were harvested, and the luciferase activities were measured by the Luc-Pair™ Duo-Luciferase Assay Kit (Genecopoeia, Guangzhou, China). Firefly luciferase activities were normalized to renilla luciferase activity. All experiments were performed in triplicate.

2.12. Tumor xenografts experiments in vivo

Six-week-old female BALB/c nude (nu/nu) mice were purchased from SJA Laboratory Animal Co., Ltd (Hunan, China; n = 42, n = 7/group). HepG2 and Huh-7 cells stably expressing sh-circZFR were subcutaneously injected into the upper left back of BALB/c nude mice. The tumor length (L) and width (W) was measured every five days thereafter and the tumor volume (V) was calculated as $V = 0.5 \times L \times W^2$. At 30 days post injection, mice were euthanized, and the tumors were excised, weighed and photographed. The animal procedures were approved by the Ethics Committees of Xiangya Hospital of Central South University

2.13. Statistical analysis

All data were analyzed by SPSS 13.0 software and presented as mean ± SD. Comparisons between two groups were performed using two-tailed Student's *t* test and multiple comparisons using one-way analysis of variance (ANOVA). The correlation between circZFR expression and clinicopathological characteristics of HCC patients was assessed by the Chi-squared test. P value of <0.05 was considered statistically significant.

3. Results

3.1. circZFR and AKT1 expression is up-regulated and miR-511 expression is down-regulated in HCC tissues and cells

We first determined the expression levels of circZFR and miR-511 by qRT-PCR and the protein levels of AKT1 by Western blotting in HCC tissues and cell lines. We found that circZFR expression was significantly increased, while miR-511 expression was significantly decreased in HCC tissues compared with that in adjacent normal tissues (Fig. 1A and B). The higher expression of circZFR was correlated with tumor size (p = 0.025) and the Tumour, Node, Metastases (TNM) stage (p = 0.021) (Table 1). Additionally, the increased levels of circZFR and decreased levels of miR-511 were also found in diverse HCC cell lines including HepG2, Bel-7402, SMMC-7721, and Huh-7, as compared with human normal hepatic cell WRL-68 (Fig. 1C and D). Western blotting results demonstrated a dramatic up-regulation of AKT1 expression in HCC cells compared to WRL-68 cells (Fig. 1E and F). These data indicated that circZFR expression was negatively correlated with miR-511 expression, and positively correlated with AKT1 expression in HCC tissues and cells. As HepG2 and Huh-7 cells showed relatively higher expression of circZFR, these two cell lines were selected for silencing of circZFR.

Table 1
Correlation between the expression levels of circZFR and the clinicopathological characteristics of HCC patients.

Clinical parameters	Cases (n)	circZFR expression		P-value (*p < 0.05)
		High (n)	Low (n)	
Gender				
Male	22	12	10	0.682
Female	8	3	5	
Age				
<60	20	9	11	0.699
≥60	10	6	4	
AFP (ng/mL)				
<400	21	9	12	0.427
≥400	9	6	3	
Tumor size (cm)				
<5	13	3	10	0.025*
≥5	17	12	5	
Differentiation grade				
Well-moderate	19	7	12	0.128
Poor-undifferentiation	11	8	3	
Cirrhosis				
Negative	4	1	3	0.598
Positive	26	14	12	
TNM stage				
I-II	11	2	9	0.021*
III-IV	19	13	6	

Abbreviations: HCC—hepatocellular carcinoma; AFP—α-fetoprotein.

3.2. circZFR up-regulates AKT1 by sponging miR-511 in HCC cells

Silencing of circZFR was performed in HCC cells to investigate its interaction with miR-511. qRT-PCR analysis confirmed that depletion of circZFR caused a significant increase in miR-511 level in both HepG2 and Huh-7 cells (Fig. 2A). Moreover, increased miR-511 level was accompanied by a concomitant decrease in AKT1 level for circZFR knockdown (Fig. 2A). Additionally, qRT-PCR analysis indicated that miR-511 inhibitor could significantly decrease miR-511 expression, while miR-511 mimics significantly increased miR-511 expression in HepG2 and Huh-7 cells (Fig. 2B). Overexpression of miR-511 could result in a significant decrease in AKT1 mRNA level, whereas miR-511 knockdown had the opposite effect in both HepG2 and Huh-7 cells (Fig. 2B). As shown in Fig. 2C and D, circZFR and AKT1 3'-UTR contained a putative binding sites of miR-511. To verify this result, we performed dual luciferase reporting assay to test the interplay between miR-511 and the predicted circZFR and AKT1 3'-UTR targeting sequences. It was notable that both circZFR and AKT1 3'-UTR showed higher luciferase activities in the presence of miR-511 inhibitor while lower luciferase activities in the presence of miR-511 mimics, by contrast, the binding site mutants of circZFR and AKT1 3'-UTR failed to display any differences with the control groups (Fig. 2E and F). These results fully revealed that circZFR could directly sponge miR-511 to counteract its suppression on AKT1, serving as a positive regulator of AKT1 and exerting its tumor-promoting effect.

3.3. Depletion of circZFR inhibits cell proliferation and induces apoptosis through up-regulating miR-511 in HCC cells

To determine whether silencing of circZFR or overexpression of miR-511 inhibit the growth of HCC cells *in vitro*, we exam-

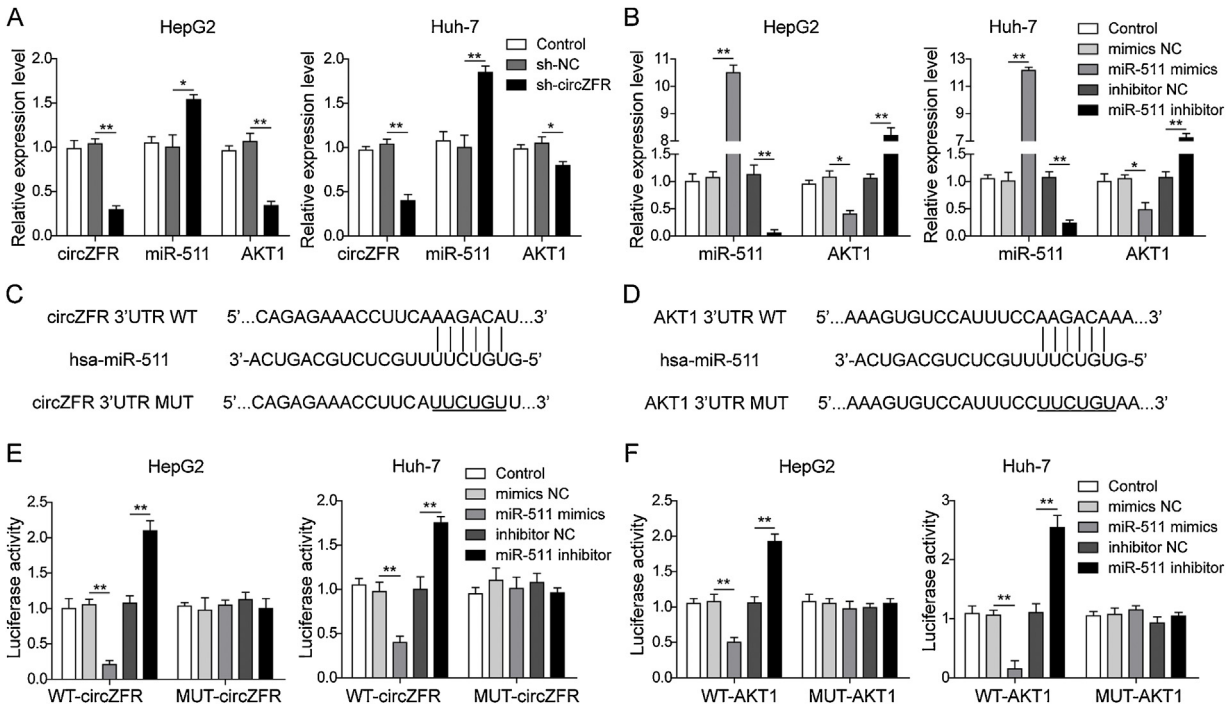

Fig. 2. Knockdown of circZFR inhibited AKT1 expression by binding to miR-511 in HCC cells. (A) The expression level of circZFR, miR-511, and AKT1 was measured by qRT-PCR in HepG2and Huh-7 cells transfected with sh-circZFR or sh-NC. (B) The expression level of miR-511 and AKT1was measured by qRT-PCR in HepG2 and Huh-7 cells transfected with miR-511 mimics, mimics NC, miR-511 inhibitor, or inhibitor NC. (C) Schematic representation of the target site in circZFR for miR-511. (D) Schematic representation of the target site in AKT1 for miR-511. miR-511 targeting sequence in circZFR (E) or AKT1 3'-UTR (F) was analyzed by dual-luciferase assay. miR-511 inhibitor or miR-511 mimics were co-transfected with firefly luciferase reporter plasmid containing human circZFR wild type (WT) or mutant (MUT) (E) or AKT1 3'-UTR WT or MUT (F) as well as the *Renilla* luciferase control reporter vector. All the results were shown as mean ± SD (n = 3), which were three separate experiments performed in triplicate. * = $p < 0.05$ and ** = $p < 0.01$.

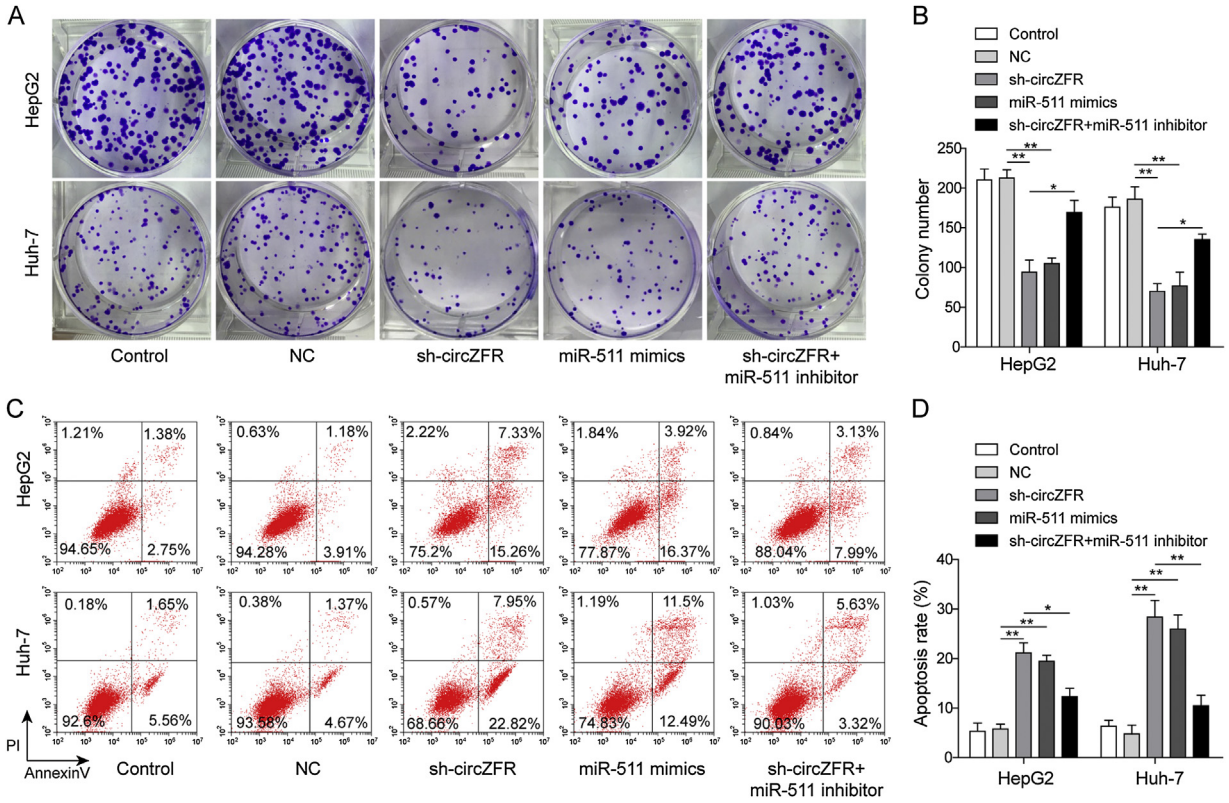

Fig. 3. Knockdown of circZFR resulted in proliferation inhibition and apoptosis induction by targeting miR-511in HCC cells. (A and B) The proliferation capacity was examined by colony formation assay in HCC cells transfected with sh-circZFR, miR-511 mimics or miR-511 inhibitor. Representative images of colonies from indicated cells were shown in A and the quantification of colony numbers in B. (C and D) The apoptosis was examined by flow cytometry following dual staining with Annexin V and propidium iodide (PI) in HCC cells transfected with sh-circZFR, miR-511 mimics or miR-511 inhibitor. The representative flow images were shown in C and the quantification of % of AnnexinV + PI + apoptotic cells in D. All the results were shown as mean ± SD (n = 3), which were three separate experiments performed in triplicate. * = $p < 0.05$ and ** = $p < 0.01$.

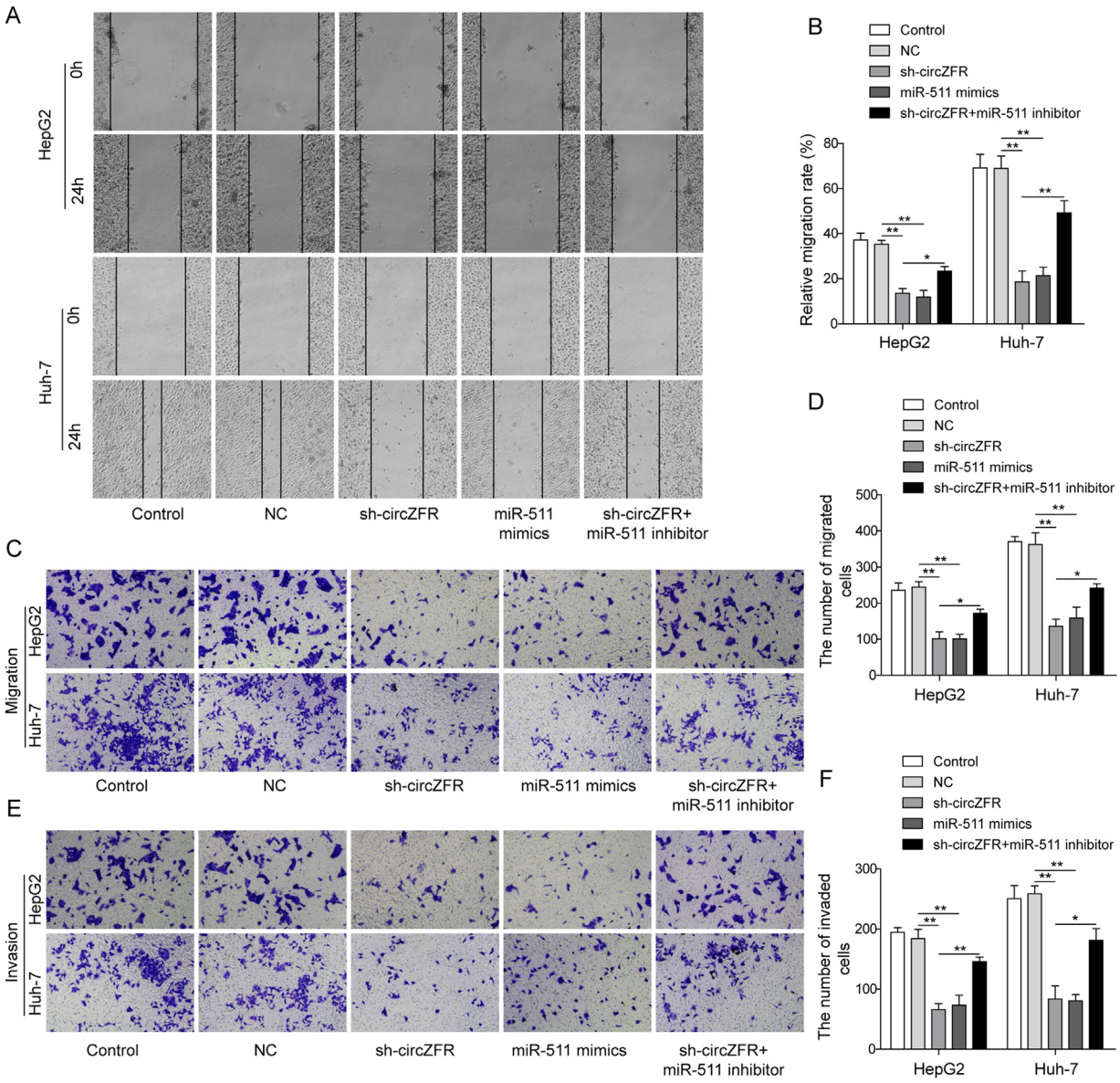

Fig. 4. Knockdown of circZFR repressed cell migration and invasion by increasing miR-511 in HCC cells. (A) The migration was examined by wound healing assays and the representative images of wound on cell monolayer were shown at 0 h and 24 h, respectively. (B) The quantification of migration rate (%) from indicated cells was shown. (C) The representative images of migrated cells were shown in transwell assay. (D) The quantification of cell migration. (E) The representative images of invaded cells were shown transwell assay. (F) The quantification of cell invasion. All the results were shown as mean ± SD (n = 3), which were three separate experiments performed in triplicate. * = $p < 0.05$ and ** = $p < 0.01$.

ined the effects of circZFR on proliferation and apoptosis of HCC cells by colony formation and flow cytometry assay. Results from colony formation assay suggested that the colony-forming activity of HepG2 and Huh-7 cells transfected with sh-circZFR was markedly less than that in control cells (Fig. 3A and B). Similarly, efficiency of colony formation was decreased upon miR-511 overexpression in HepG2 and Huh-7 cells (Fig. 3A and B). Furthermore, knockdown of circZFR markedly accelerated cell apoptosis in both HepG2 and Huh-7 cells (Fig. 3C and D). The effect of miR-511 overexpression on cell apoptosis was similar to that of circZFR knockdown (Fig. 3C and D). In order to functionally confirm that circZFR promotes HCC progression by regulating miR-511, we performed rescue experiments by co-transfecting with sh-circZFR and miR-511 inhibitor in HCC cells. Results from both colony formation assays and flow cytometry analysis revealed that miR-511 inhibitor partially reversed the effects of circZFR silencing on cell growth and apoptosis *in vitro* (Fig. 3A–D). These data suggested that circZFR promoted cell proliferation and inhibited cell apoptosis through inhibiting miR-511 in HCC.

3.4. Depletion of circZFR suppresses cell migration and invasion through increasing miR-511 in HCC cells

We next explored the effects of circZFR and miR-511 on motility of HCC cells, utilizing a classic *in vitro* wound-healing model. Treatment of HepG2 and Huh-7 cells with sh-circZFR markedly decreased the cell migration into the denuded area, as evidenced by a slower closing of scratch wound compared to sh-NC group (Fig. 4A and B). Similarly, the wound filling was evidently decelerated in HepG2 and Huh-7 cells transfected with miR-511 mimics (Fig. 4A and B). Moreover, knockdown of circZFR remarkably reduced cell migration and invasion compared to sh-NC group, as determined by transwell assays (Fig. 4C–F). Overexpression of miR-511 also force fully decreased the number of migrated and invaded cells

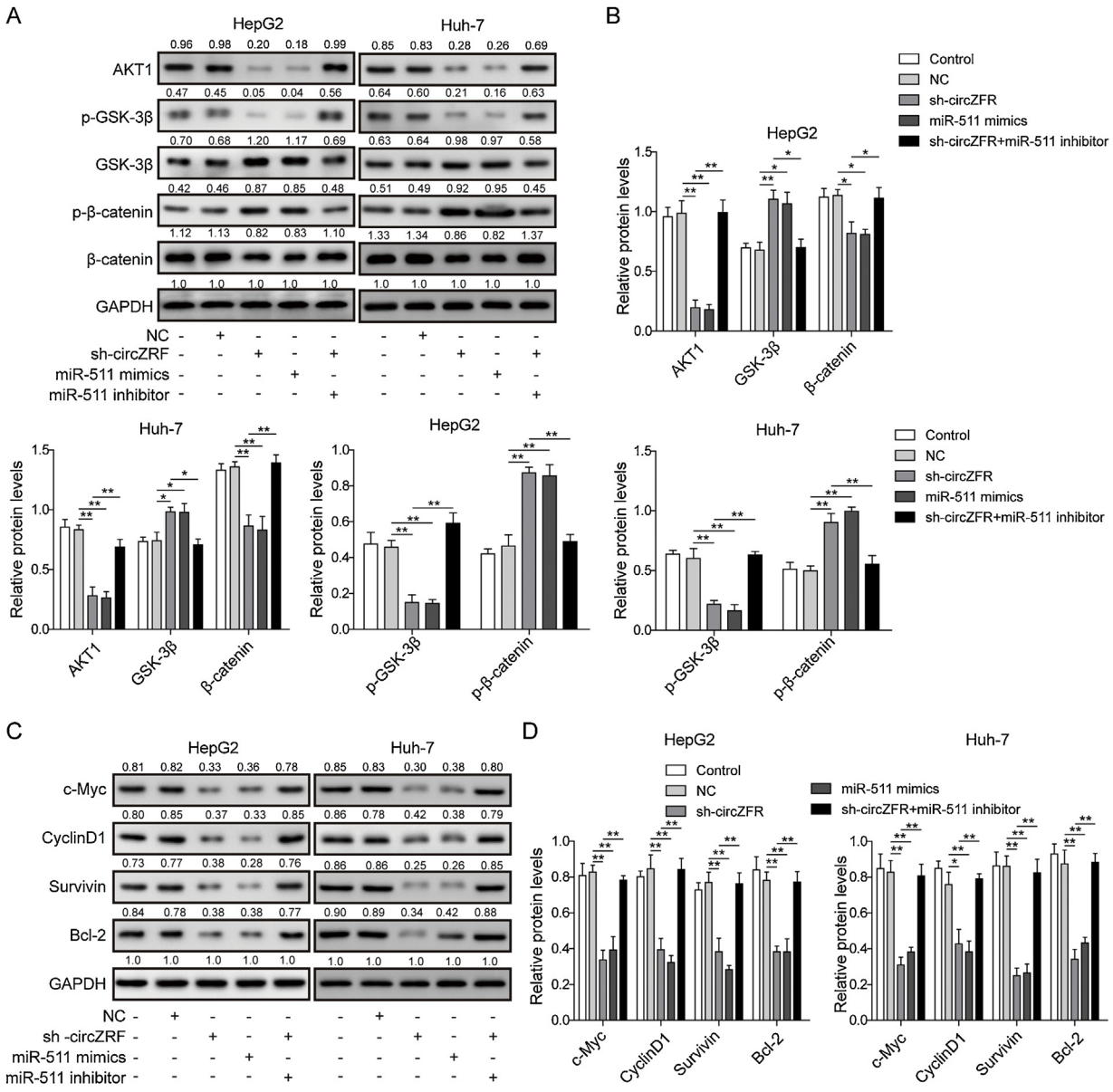

Fig. 5. Knockdown of circZFR suppressed AKT1/β-catenin signaling pathway by directly up-regulating miR-511 in HCC cells. (A) The protein levels of AKT1, GSK-3β, p-GSK-3β, β-catenin and p-β-catenin were detected by western blotting in HepG2 and Huh-7 cells treated with sh-circZFR, miR-511 mimics or miR-511 inhibitor. (B) The quantification of relative protein level as a ratio to that of GAPDH (internal control). (C) The protein levels of c-Myc, cyclin D1, Survivin and Bcl-2 were detected by western blotting in HepG2 and Huh-7 cells treated with c sh-circZFR, miR-511 mimics, or miR-511 inhibitor. (D) The quantification of relative protein level as a ratio to that of GAPDH (internal control). All the results were shown as mean ± SD (n = 3), which were three separate experiments performed in triplicate. * = p < 0.05 and ** = p < 0.01.

(Fig. 4C–F). Notably, the suppressive effects of circZFR silencing on cell migration and invasion were partially rescued by miR-511 inhibitor in HepG2 and Huh-7 cells (Fig. 3A-F). Collectively, these findings fully demonstrated that circZFR potentiated cell migration and invasion by down-regulating miR-511 in HCC.

3.5. *circZFR activates AKT1/ β-catenin signaling pathway* via *targeting miR-511 in HCC cells*

We noticed that knockdown of circZFR significantly down-regulated the protein expression level of AKT1 (Fig. 5A and B). This was accompanied by inhibition of the GSK-3β/β-catenin signaling pathway, as indicated by reduced expression of phosphorylation of GSK-3β (p-GSK-3β) and β-catenin and increased expression of GSK-3β and phosphorylation of β-catenin (p-β-catenin) (Fig. 5A and B). We also found that the expression level of several proliferation-related proteins c-Myc and cyclin D1 and anti-apoptotic proteins Survivin and Bcl-2 were strongly down-regulated in HepG2 and Huh-7 cells transfected with sh-circZFR and miR-511 mimics (Fig. 5C and D). Notably, the above changes induced by circZFR depletion were partially abrogated by miR-511 inhibitor in HepG2 and Huh-7 cells (Fig. 5A–D). These data indicated that circZFR activated AKT1/β-catenin signaling pathway by directly down-regulating miR-511 in HCC cells.

3.6. *Knockdown of circZFR inhibits xenograft growth* via *regulating miR-511/AKT1 axis* in vivo

To explore the *in vivo* activities of circZFR during HCC development, we established xenografts from HepG2 and Huh-7 cells. By monitoring the xenograft growth, we found that sh-circZFR-transfected cells generated xenografts significantly lower in both

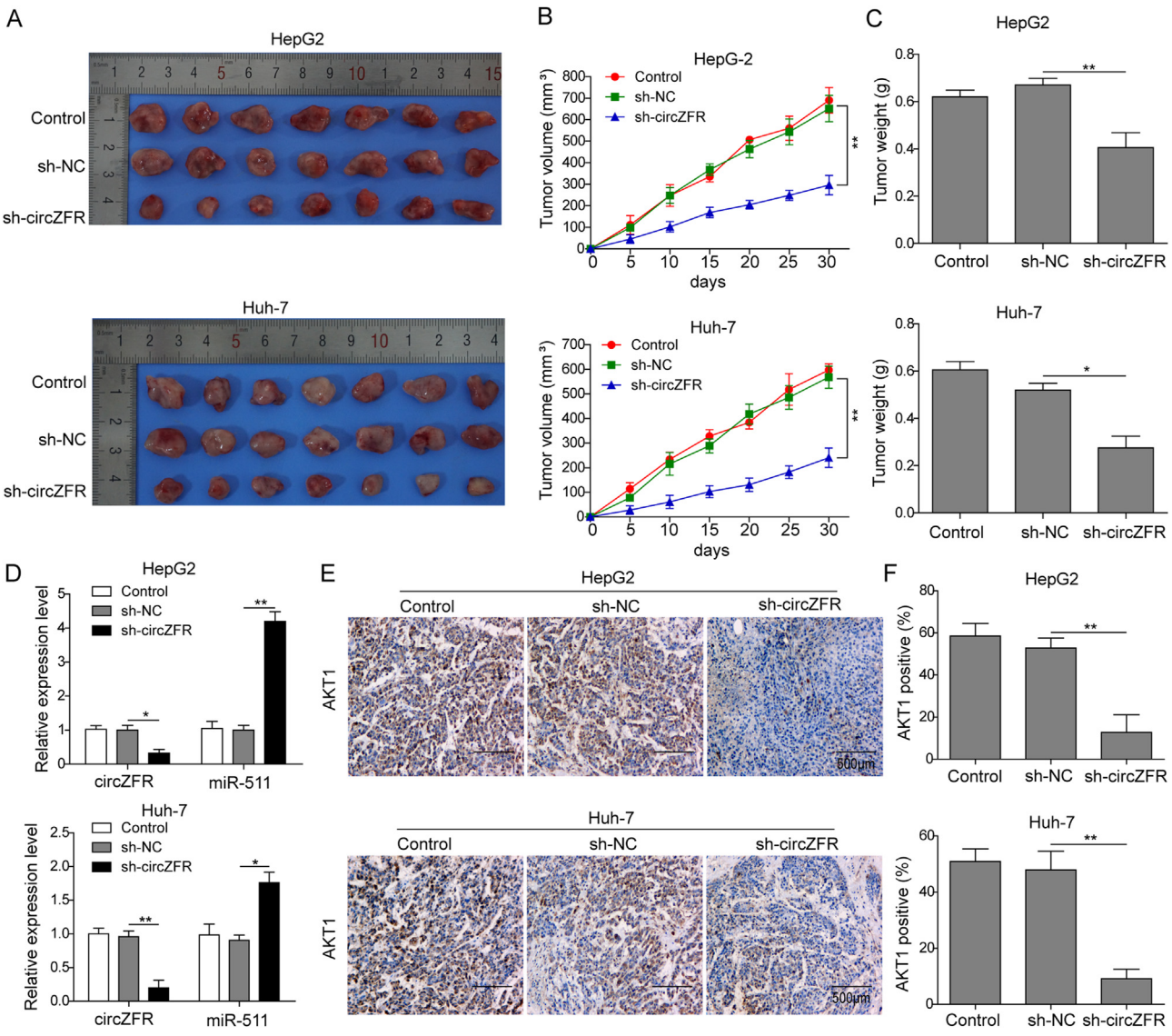

Fig. 6. circZFR promoted tumorigenesis *via* regulating miR-511/AKT1 axis *in vivo*. (A) Representative pictures of isolated xenografts were shown. (B) Tumor sizes measured every five days with electronic caliper. (C) Weights of tumors harvested from mice at the end of experiments. (D) The expression level of circZFR and miR-511 in xenografts was measured by qRT-PCR. (E) IHC staining analysis of AKT1. Scale bar: 500 μm. (F) The positive signals for AKT1 were quantified. The results were shown as mean ± SD (n = 3), which were three separate experiments performed in triplicate. * = $p < 0.05$ and ** = $p < 0.01$.

size and weight in the two cell lines (Fig. 6A–C). The expression level of circZFR was markedly reduced while miR-511 was significantly increased in xenografts derived from sh-circZFR in both HepG2 and Huh-7 cells (Fig. 6D). Moreover, IHC revealed that circZFR silencing decreased the proportion of AKT1-positive cells (Fig. 6E and F). These results demonstrated that circZFR could promote xenografts growth through the miR-51/AKT1 axis *in vivo*.

4. Discussion

As a type of novel non-coding RNAs, a growing body of evidence indicates that circRNAs may serve as potential biomarkers and regulators for cancers [6]. circZFR is a newly identified non-coding circle RNA, which has been proposed as a prognostic indicator and therapeutic target in HCC [15]. Previous study revealed that circZFR initiated the development of lung cancer through repressing miR-4302 to facilitate MYC expression [31]. By contrast, circZFR suppressed cell proliferation and promoted apoptosis in gastric cancer by modulating PTEN *via* sponging miR-130a/miR-107 [32]. This indicates that circZFR plays complex dual roles as an inhibitor and promoter of tumor progression depending on the cellular circumstances. However, the role and underlying mechanism of circZFR in HCC remains unclear. In the current study, we presented for the first time the expression, functions, and potential molecular mechanism of circZFR in HCC progression. Our study demonstrated that circZFR was up-regulated in HCC tissues and cells. Importantly, loss-of-function experiments revealed that circZFR depletion suppressed cell proliferation, migration and invasion, and induced cell apoptosis. Importantly, we confirmed the functions of circZFR in HCC *in vivo* by building nude mice model. Our findings demonstrate that circZFR is an oncogene in HCC and blockage of circZFR may be a promising strategy for HCC treatment.

Accumulating reports demonstrate that circRNAs can act as competing endogenous RNAs (ceRNAs) for miRNA targets [26], and ceRNAs can seclude miRNAs, thereby protecting their target RNAs from repression [33]. In this context of HCC, several circRNA-miRNA interactions have been identified to be critical contributors to its initiation and progression. For instance, circMTO1, which was down-regulated in HCC and was an indicator of shortened survival, inhibited tumor progression by deactivat-

ing miR-9-mediateddown-regulation of p21 [8]. circHIPK3 and hsa_circ_0016788 were up-regulated in HCC and promoted cell proliferation by function as ceRNA for the miR-124 family [11–13]. Based on the bioinformatics data and prior findings [15], we assumed that circZFR might be a target gene of miR-511 in HCC cells. Consistently with previous studies [23–25], we found that miR-511 was significantly down-regulated in HCC tissues and cells. In addition, the expression of miR-511 was negatively regulated by circZFR in HCC cells. We carried out luciferase reporter assay and found that circZFR could directly bind to miR-511. More importantly, rescue experiments *in vitro* demonstrated that miR-511 was a key mediator of circZFR in HCC cell activities. These findings strongly revealed that circZFR may act as an miR-511 sponge in HCC.

AKT1 is known to be contributor to HCC tumorigenesis, and has been described as an important target of several miRNAs in HCC [29,30]. AKT1 is a crucial receptor for activation of highly oncogenic Wnt/β-catenin signal pathway [27], which is closely linked to HCC cell proliferation and migration [34,35]. GSK-3β, a known phosphorylation substrate of AKT1, behaves as part of the circuitry; inactivation of GSK-3β by Ser9 phosphorylation induced by phosphorylation of AKT1 at Ser473 could promote accumulation of β-catenin and ultimately activate the Wnt/β-catenin signaling pathway [36–38]. Moreover, previous studies showed that miR-511 acts as a negative regulator of PI3K/AKT pathways in HCC [24]. In our study, we found that AKT1 levels were significantly up-regulated in HCC cells, and our luciferase reporter gene indicated that AKT1 was a target gene of miR-511. Western blot analysis showed that knockdown of circZFR and overexpression of miR-511 could repress AKT1-mediated GSK-3β/β-catenin signaling pathway. In addition, the proliferation-associated proteins including c-Myc, cyclin D1, surviving and Bcl-2 were significantly decreased in HCC cells transfected with sh-circZFR and miR-511 mimics. In support of these observations, shRNA-mediated knockdown of circZFR suppressed tumor progression *in vivo*. These results fully illuminated that circZFR promoted multiple malignant phenotypes *via* directly down-regulating miR-511 to activate AKT1/β-catenin signal pathway in HCC.

In conclusion, we determined the expression and functions of circZFR in HCC for the first time. circZFR regulates the proliferation, migration and invasion of HCC cells by targeting miR-511 to activate AKT/β-catenin signaling pathway. *In vivo* study confirmed the tumor-promoting role of circZFR in HCC. Further understanding of the circZFR-miR-511-AKT1 axis should provide new insight into the pathogenesis of disease and the development of new strategies to treat HCC in the future.

Conflict of interest

None declared.

Acknowledgements

We would like to give our sincere gratitude to the reviewers for their constructive comments.

References

[1] Torre LA, Bray F, Siegel RL, Ferlay J, Lortet-Tieulent J, Jemal A. Global cancer statistics. CA Cancer J Clin 2012;2015(65):87.
[2] Chen W, Zheng R, Baade PD, Zhang S, Zeng H, Bray F, et al. Cancer statistics in China. CA Cancer J Clin 2015;2016(66):115.
[3] Schottenfeld D, Fraumeni JFU. Cancer epidemiology and prevention. Oxford University Press; 2006.
[4] Shen S, Lin Y, Yuan X, Shen L, Chen J, Chen L, et al. Biomarker microRNAs for diagnosis, prognosis and treatment of hepatocellular carcinoma: a functional survey and comparison. Sci Rep 2016;6:38311.
[5] Ebbesen KK, Hansen TB, Kjems J. Insights into circular RNA biology. RNA Biol 2017;14:1035.
[6] Li Y, Zheng Q, Bao C, Li S, Guo W, Zhao J, et al. Circular RNA is enriched and stable in exosomes: a promising biomarker for cancer diagnosis. Cell Res 2015;25:981.
[7] Qu S, Yang X, Li X, Wang J, Gao Y, Shang R, et al. Circular RNA: a new star of noncoding RNAs. Cancer Lett 2015;365:141.
[8] Han D, Li J, Wang H, Su X, Hou J, Gu Y, et al. Circular RNA circMTO1 acts as the sponge of microRNA-9 to suppress hepatocellular carcinoma progression. Hepatology 2017;66:1151.
[9] Yao Z, Luo J, Hu K, Lin J, Huang H, Wang Q, et al. ZKSCAN1 gene and its related circular RNA (circZKSCAN1) both inhibit hepatocellular carcinoma cell growth, migration, and invasion but through different signaling pathways. Mol Oncol 2017;11:422.
[10] Yu J, Xu QG, Wang ZG, Yang Y, Zhang L, Ma JZ, et al. Circular RNA cSMARCA5 inhibits growth and metastasis in hepatocellular carcinoma. J Hepatol 2018;68:1214.
[11] Zheng Q, Bao C, Guo W, Li S, Chen J, Chen B, et al. Circular RNA profiling reveals an abundant circHIPK3 that regulates cell growth by sponging multiple miRNAs. Nat Commun 2016;7:11215.
[12] Chen G, Shi Y, Liu M, Sun J. circHIPK3 regulates cell proliferation and migration by sponging miR-124 and regulating AQP3 expression in hepatocellular carcinoma. Cell Death Dis 2018;9:175.
[13] Guan Z, Tan J, Gao W, Li X, Yang Y, Li X, et al. Circular RNA hsa_circ_0016788 regulates hepatocellular carcinoma tumorigenesis through miR-486/CDK4 pathway. J Cell Physiol 2018;234:500.
[14] Huang XY, Huang ZL, Xu YH, Zheng Q, Chen Z, Song W, et al. Comprehensive circular RNA profiling reveals the regulatory role of the circRNA-100338/miR-141-3p pathway in hepatitis B-related hepatocellular carcinoma. Sci Rep 2017;7:5428.
[15] Ren S, Xin Z, Xu Y, Xu J, Wang G. Construction and analysis of circular RNA molecular regulatory networks in liver cancer. Cell Cycle 2017;16:2204.
[16] Romero-Cordoba S, Salido-Guadarrama I, Rodriguez-Dorantes M, Hidalgo-Miranda A. miRNA biogenesis: biological impact in the development of cancer. Cancer Biol Ther 2014;15:1444.
[17] Chen L, Yao H, Wang K, Liu X. Long non-coding RNA MALAT1 regulates ZEB1 expression by sponging miR-143-3p and promotes hepatocellular carcinoma progression. J Cell Biochem 2017;118:4836.
[18] Chen GS, Zhou N, Li JQ, Li T, Zhang ZQ, Si ZZ. Restoration of miR-20a expression suppresses cell proliferation, migration, and invasion in HepG2 cells. Onco Targets Ther 2016;9:3067.
[19] Yang H, Fang F, Chang R, Yang L. MicroRNA-140-5p suppresses tumor growth and metastasis by targeting transforming growth factor beta receptor 1 and fibroblast growth factor 9 in hepatocellular carcinoma. Hepatology 2013;58:205.
[20] Squadrito ML, Pucci F, Magri L, Moi D, Gilfillan G, iA Ranghett, et al. miR-511-3p modulates genetic programs of tumor-associated macrophages. Cell Rep 2012;1:141.
[21] Fang Z, Zhang L, Liao Q, Wang Y, Yu F, Feng M, et al. Regulation of TRIM24 by miR-511 modulates cell proliferation in gastric cancer. J Exp Clin Cancer Res 2017;36:17.
[22] Zhang F, Wu Z. Significantly altered expression of miR-511-3p and its target AKT3 has negative prognostic value in human prostate cancer. Biochimie 2017;140:66.
[23] Wang W, Zhao L, Tan Y, Ren H, Qi Z. MiR-138 induces cell cycle arrest by targeting cyclin D3 in hepatocellular carcinoma. Carcinogenesis 2012;33:1113.
[24] Cao G, Dong W, Meng X, Liu H, Liao H, Liu S. MiR-511 inhibits growth and metastasis of human hepatocellular carcinoma cells by targeting PIK3R3. Tumour Biol 2015;36:4453.
[25] Zhang J, Chong C, Chen G, Lai P. A seven-microRNA expression signature predicts survival in hepatocellular carcinoma. PLoS One 2015;10:e0128628.
[26] Cui X, Wang J, Guo Z, Li M, Li M, Liu S, et al. Emerging function and potential diagnostic value of circular RNAs in cancer. Mol Cancer 2018;17:123.
[27] Manning BD, Toker A. AKT/PKB signaling: navigating the network. Cell 2017;169:381.
[28] Zhang Y, Guo X, Yang M, Yu L, Li Z, Lin N. Identification of AKT kinases as unfavorable prognostic factors for hepatocellular carcinoma by a combination of expression profile, interaction network analysis and clinical validation. Mol Biosyst 2014;10:215.
[29] Zhang Y, Guo X, Xiong L, Yu L, Li Z, Guo Q, et al. Comprehensive analysis of microRNA-regulated protein interaction network reveals the tumor suppressive role of microRNA-149 in human hepatocellular carcinoma via targeting AKT-mTOR pathway. Mol Cancer 2014;13:253.
[30] Shen G, Rong X, Zhao J, Yang X, Li H, Jiang H, et al. MicroRNA-105 suppresses cell proliferation and inhibits PI3K/AKT signaling in human hepatocellular carcinoma. Carcinogenesis 2014;35:2748.
[31] Liu W, Ma W, Yuan Y, Zhang Y, Sun S. Circular RNA hsa_circRNA_103809 promotes lung cancer progression via facilitating ZNF121-dependent MYC expression by sequestering miR-4302. Biochem Biophys Res Commun 2018;500:846.
[32] Liu T, Liu S, Xu Y, Shu R, Wang F, Chen C, et al. Circular RNA-ZFR inhibited cell proliferation and promoted apoptosis in gastric Cancer by sponging miR-130a/miR-107 and modulating PTEN. Cancer Res Treat 2018;50:1396.
[33] Tay Y, Kats L, Salmena L, Weiss D, Tan S, Ala U, et al. Coding-independent regulation of the tumor suppressor PTEN by competing endogenous mRNAs. Cell 2011;147:344.
[34] Li Z, Xue TQ, Yang C, Wang YL, Zhu XL, Ni CF. EGFL7 promotes hepatocellular carcinoma cell proliferation and inhibits cell apoptosis through increasing

CKS2 expression by activating Wnt/beta-catenin signaling. J Cell Biochem 2018, http://dx.doi.org/10.1002/jcb.27375 [Epub ahead of print].
[35] Wang Y, Sun L, Wang L, Liu Z, Li Q, Yao B, et al. Long non-coding RNA DSCR8 acts as a molecular sponge for miR-485-5p to activate Wnt/beta-catenin signal pathway in hepatocellular carcinoma. Cell Death Dis 2018;9:851.
[36] Moroi AJ, Watson SP. Akt and mitogen-activated protein kinase enhance C-type lectin-like receptor 2-mediated platelet activation by inhibition of glycogen synthase kinase 3alpha/beta. J Thromb Haemost 2015;13:1139.
[37] Yang K, Wang X, Zhang H, Wang Z, Nan G, Li Y, et al. The evolving roles of canonical WNT signaling in stem cells and tumorigenesis: implications in targeted cancer therapies. Lab Invest 2016;96:116.
[38] Conde-Perez A, Gros G, Longvert C, Pedersen M, Petit V, Aktary Z, et al. A caveolin-dependent and PI3K/AKT-independent role of PTEN in beta-catenin transcriptional activity. Nat Commun 2015;6:8093.